

TWO DIMENSIONAL SYNCHROTRON RADIATION INTERFEROMETRY AT PETRA III

A. I. Novokshonov, A. P. Potylitsyn, Tomsk Polytechnic University (TPU), Tomsk, Russia
G. Kube, Deutsches Elektronen-Synchrotron (DESY), Hamburg, Germany

Abstract

Synchrotron radiation interferometry is widely used at modern light sources in order to measure transverse electron beam sizes. The technique is based on probing the spatial coherency of synchrotron radiation in the visible spectral region. The light source PETRA III at DESY (Hamburg, Germany) used this type of interferometer since several years in order to resolve vertical emittances of about 10 pm.rad. In order to overcome some inherent disadvantages in this setup, a new optical diagnostics beamline was recently commissioned with a two-dimensional interferometer, thus allowing to measure beam sizes in both transverse planes simultaneously. This contribution summarizes the status of the interferometer setup and describes studies concerning the possibility to increase the sensitivity on small beam sizes using an intensity imbalance technique.

INTRODUCTION

Synchrotron radiation (SR) interferometry in the visible spectral region is a common method to measure transverse beam sizes down to the few micrometer level at 3rd generation light sources. In order to overcome some inherent disadvantages in the previous interferometer setup at PETRA III, a new optical beamline for two-dimensional SR interferometry was recently commissioned and is now in operation for simultaneous online monitoring of transverse beam emittances in both planes [1]. However, one of the interferometric limitations is the dynamic range when measuring ultra low emittance beams with modulation depths (visibilities) close to unity. In order to circumvent this limitation, T. Mitsuhashi proposed to introduce an intensity imbalance in one of the light paths, and the method was already tested successfully at the Australian Synchrotron and at the ATF2 (KEK, Japan) [2]. While these interferometers like most other setups in use are designed for profile diagnostics in only one plane (to the authors knowledge, the operation of a two-dimensional SR interferometer was reported so far only from the SPring-8 light source in Japan [3]), the idea was to combine the intensity imbalance method with the two-dimensional interferometer setup and to study sensitivity and stability both theoretically and experimentally. In the following, the status of these investigations is presented.

INTERFEROMETER PRINCIPLE

The principle of the interferometric method is based on the investigation of the spatial coherence of SR. In order to quantify the coherence properties, usually the first order degree of mutual spatial coherence $\gamma(D)$ is used (c.f. for

example Ref. [4]) with D the distance between two wavefront dividing apertures, see Fig. 1. In case of circular apertures (pinholes), the intensity of the interference pattern (interferogram) in the detector plane is given by [5]

$$I(y_0) = I_0 \left[\frac{J_1 \left(\frac{2\pi a y_0}{\lambda R} \right)}{\frac{2\pi a y_0}{\lambda R}} \right]^2 \left[1 + |\gamma| \cos \left(\frac{2\pi D}{\lambda_0 R} + \varphi \right) \right] \quad (1)$$

with a the pinhole radius, D and R as indicated in Fig. 1, λ_0 the wavelength of observation, and I_0 the sum of the incoherent intensities from the pinholes. If the condition of Fraunhofer diffraction (i.e. far-field limit) holds, the van Cittert-Zernicke theorem [6] relates the degree of coherence γ with the normalized source distribution $f(y)$:

$$\gamma(\nu) = \int dy f(y) \exp(-i2\pi\nu y), \quad (2)$$

where $\nu = \frac{D}{\lambda_0 R_0}$ denotes the spatial frequency. The beam size information is encoded in the interferogram such that as smaller the beam size, as deeper the modulation depth of the interference pattern. In case of an ideal point source, the intensity in the minima of the pattern would amount to $I_{min} = 0$, resulting in a visibility of $V = \frac{I_{max} - I_{min}}{I_{max} + I_{min}} = |\gamma| = 1$. The visibility of an extended source will always have a visibility $V < 1$.

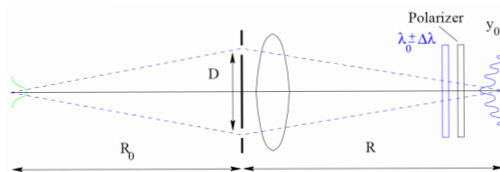


Figure 1: Principle setup for interferometric beam size measurements.

If the beam shape $f(y)$ is known to be normal distributed with width σ_y , the integral in Eq. (2) can be solved analytically which results in the following equation

$$\sigma_y = \frac{\lambda_0 R_0}{\pi D} \sqrt{\frac{1}{2} \ln \frac{1}{|\gamma(D)|}}, \quad (3)$$

by which the beam size can directly be determined, while $\gamma(D)$ has to be fitted from the recorded interferogram.

In the case of a 2-D interferometer, 4 pinholes instead of 2 are used as shown in Fig. 2 which results in interference patterns in both transverse directions, c.f. Fig. 3. Taking the central cuts in both planes from a measured interferogram

Fig. 3 (right) and applying Eq. 1 with the aperture distances $D_{x,y}$, it is possible to extract the degrees of coherence $\gamma_{x,y}$ and convert them to the corresponding transverse beam sizes $\sigma_{x,y}$ according to Eq. 3. A comprehensive overview and a detailed description about the 2-D SR interferometer theory can be found in Ref. [3].

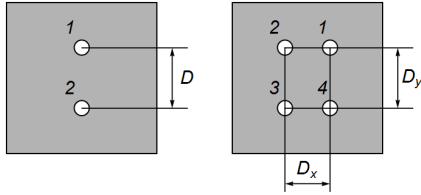


Figure 2: 1-D (left) and 2-D (right) aperture mask geometry.

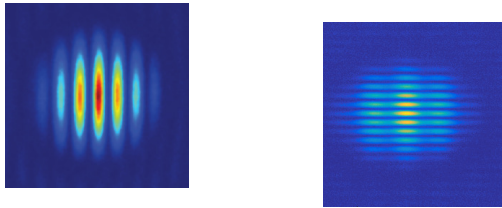


Figure 3: Measured 1-D (left) and 2-D (right) interferogram.

INTENSITY IMBALANCE

Limitation of a conventional interferometer is the dynamic range when measuring ultra low emittance beams with visibilities close to unity such that the troughs are located in or close to the noise floor of the CCD camera recording the interferograms. In this case it is the noise floor which determines the minimum beam size that can be measured. Besides the usage of a low noise camera, it is possible to improve the situation by introducing an intensity imbalance in one of the light paths as successfully demonstrated in Ref. [2]. For a 1-D interferometer setup this can be achieved by attenuating the light passing one of the apertures with a filter of pre-defined attenuation coefficient. In order to get the information about the true beam size from the measured visibility V , the degree of coherence in Eq. (3) has to be corrected according to

$$|\gamma| = \frac{1 + K}{2\sqrt{K}} V \tag{4}$$

with the imbalance ratio $K = I_1/I_2$ [2]. In the case of balanced intensities, $K = 1$ and $|\gamma| = V$.

For illustration purposes Fig. 4 shows calculated 1-D interferograms based on the SRW code [7] without (left) and with (right) intensity imbalance using a factor of $K = 4$, i.e. the SR intensity passing the first pinhole is 4 times higher than the one from the second pinhole. As can be seen, the troughs in the interferogram are raised up. Both interferograms were fitted in order to determine the visibility V and $|\gamma|$ which was then transformed into a beam size according to Eq. (3). The resulting parameters are quoted in the figure insert and agree well in both cases.

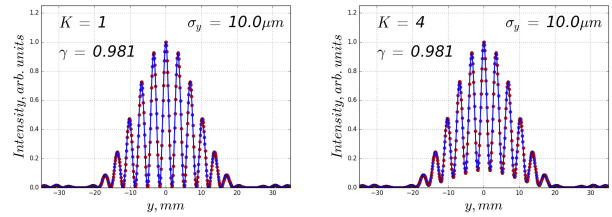


Figure 4: Calculated interferograms (red points) without (left) and with intensity imbalance (right) together with a fit (blue curve). The fitted and corrected $|\gamma|$ values together with the derived beam sizes are indicated in the figure.

In the case of a 2-D interferometer intensity imbalance in one plane is achieved by attenuating 2 of the 4 pinholes. As an example, if imbalance has to be introduced in the vertical plane, the intensity passing through the pinholes 1 and 2 should equally be attenuated (c.f. Fig. 2 right).

In the next step the possibility is discussed to introduce intensity imbalance simultaneously in both planes. This can be achieved by the scheme introduced in Fig. 5. For simplicity, pinhole 2 is completely covered such that no radiation can pass through. In this case $K_x = (I_1 + I_4)/(I_2 + I_3) = 2$ and $K_y = (I_3 + I_4)/(I_1 + I_2) = 2$, i.e. intensity imbalance is introduced in both planes.

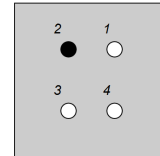


Figure 5: Scheme of 2-D imbalance technique in both planes.

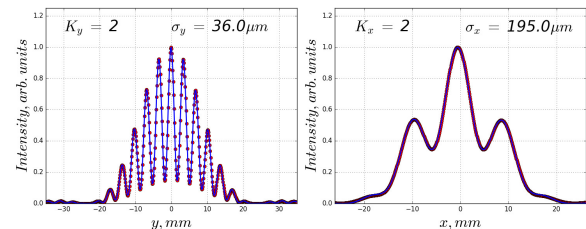


Figure 6: Calculated vertical (left) and horizontal (right) interferograms (red points) from an imbalanced 2-D interferometer with one pinhole masked together with the fit (blue curve) based on Eq. (1).

For better illustration this case was also investigated with SRW. Figure 6 shows calculated horizontal and vertical interferograms from a 2-D imbalanced interferometer with one pinhole masked, assuming input beam sizes of $\sigma_x = 174\mu\text{m}$ and $\sigma_y = 10\mu\text{m}$. Again the calculated interferograms are fitted based on Eq. (1), and the extracted beam sizes are indicated in the figure. As can be seen from this comparison, the extracted beam sizes are much larger than the ones used as input for the calculation.

In order to study the origin of this discrepancy, based on the 2-D SR interferometer theory described in Ref. [3] the following formula was derived for a 2-D imbalanced interferometer with one masked pinhole

$$\begin{aligned} \tilde{I}(x, y) = I_0 & \left(\frac{J_1 \{ (\pi d / \lambda_0) [(x/R)^2 + (y/R)^2]^{1/2} \}}{(\pi d / \lambda_0) [(x/R)^2 + (y/R)^2]^{1/2}} \right)^2 \times \\ & \left(\frac{3}{2} + V_{14} \cos \left[\frac{2\pi D_y}{\lambda_0 R} y \right] + V_{34} \cos \left[\frac{2\pi D_x}{\lambda_0 R} x \right] + \right. \\ & \left. V_{13} \cos \left[\frac{2\pi D_x}{\lambda_0 R} x + \frac{2\pi D_y}{\lambda_0 R} y \right] \right) \end{aligned} \quad (5)$$

with V_{14} , V_{34} , V_{13} the visibilities of pinholes 1-4, 3-4, and 1-3. Interferogram calculations based on Eq. (5) agree very well with the SRW calculations, thus confirming the previous results. However, advantage of this description is to get better insight in the required fit functions. Assuming as before that the fit will be carried out at the central cut of the 2-D interferogram (i.e. in the horizontal plane at $y = 0$ and vice versa), according to Eq. (5) the required fit function reads

$$\tilde{I}(x) = I_0 \left(\frac{J_1(d\xi)}{d\xi} \right)^2 \left(\frac{3}{2} + \cos[2\xi D_x] (V_{34} + V_{13}) \right) \quad (6)$$

with $\xi = \frac{\pi x}{\lambda_0 R}$. From the inspection of Eq. (6) it is obvious that in the case of an imbalanced setup, the interference in the horizontal plane does not depend only on the visibility V_{34} in this plane, but also on the "diagonal" visibility V_{13} , thus explaining the discrepancy between input and extracted beam sizes in Fig. 6.

EXPERIMENTAL INVESTIGATION

In a first experimental test an imbalanced 2-D interferometer with attenuation in only one plane was studied. For this purpose commercial neutral density filters were used which consisted of a 2 mm thick glass substrate with one half covered by black dots, the dot density defining the optical density (OD). This kind of split filter was used in order to introduce only an attenuation, but not an additional phase shift. Two filters with $OD \approx 0.38$ and 0.95 were tested in the experiment. Vertical beam size measurements with the $OD = 0.38$ filter are shown in Fig. 7. Besides the oscillatory structure whose origin is still under investigation, the measured beam sizes are about a factor of 5 higher than the expected ones in the order of $\sigma_y = 10 - 15 \mu\text{m}$. Fig. 8 shows a similar measurement for the $OD = 0.95$ attenuator, resulting in an about 3 times larger beam size than the expected one. The reason of this discrepancy in beam size determination is still under investigation, but a possible explanation would be the type of attenuation in use which is managed by the density of black dots: for interferometric measurements, a homogeneous attenuation seems to be more suitable.

First measurements with the 2-D imbalanced setup in both transverse planes (i.e. one pinhole masked) are underway, showing the expectation based on the SRW calculations that both transverse beam size measurements will overestimate the real ones.

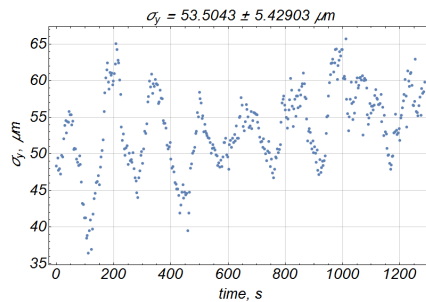


Figure 7: Vertical size measurements with $OD = 0.38$ attenuator.

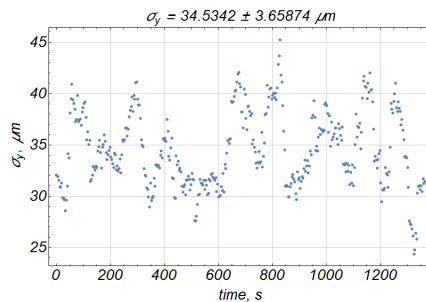


Figure 8: Vertical size measurements with $OD = 0.95$ attenuator.

SUMMARY AND OUTLOOK

The present report summarizes first theoretical and experimental investigations of an intensity imbalance technique applied to a 2-D interferometer. The results indicate that (1) the imbalance technique should be investigated more carefully using filters based on homogeneous attenuation, and that (2) the extraction of beam size information from measured interferograms will not be possible using common interferometric formulas. Eq. (6) indicates that the effective visibility depends not only on the visibility in the plane under investigation, but also on the "diagonal" one. In this situation it is not possible to extract beam sizes from a single 1-D fit of the central cut of a 2-D interferogram, a full 2-D fit seems to be better suited.

REFERENCES

- [1] A.I. Novokshonov, A.P. Potylitsyn, G. Kube, M. Pelzer and G. Priebe, Proc. of IBIC'16, Barcelona, Spain, September 2016, <http://ibic2016.vrws.de/papers/wepg76.pdf>.
- [2] M.J. Boland, T. Mitsuhashi, T. Naito and K.P. Wootton, Proc. IBIC'12, Tsukuba, Japan, WECC03, p. 566 – 570 (2012).
- [3] M. Masaki and S. Takano, J. Sync. Rad. **10** (2003), 295.
- [4] M. Born and E. Wolf, Principles of Optics, Pergamon Press Ltd., New York, 1980.
- [5] L. Torino and U. Iriso, Proc. IBIC'15, Melbourne, Australia, September 2015, PS17, p. 428 – 432 (2015).
- [6] P. H. Van Cittert, Physica **1**, 201 (1934). F. Zernike, Physica **5**, 785 (1938).
- [7] O. Chubar and P. Elleaume, Proceedings of the EPAC98, Stockholm, Sweden, June 1998, p.1177–1179 (1998).